

# Effects of birefringence on Fizeau interferometry that uses a polarization phase-shifting technique

Chunyu Zhao, Dongyel Kang, and James H. Burge

Interferometers that use different states of polarization for the reference and the test beams can modulate the relative phase shift by using polarization optics in the imaging system. Thus the interferometer can capture simultaneous images that have a fixed phase shift, which can be used for phase-shifting interferometry. As all measurements are made simultaneously, the interferometer is not sensitive to vibration. Fizeau interferometers of this type have an advantage compared with Twyman–Green-type systems because they are common-path interferometers. However, a polarization Fizeau interferometer is not strictly common path when both wavefronts are transmitted by an optic that suffers from birefringence. The two polarized beams see different phases owing to birefringence; as a result, an error can be introduced in the measurement. We study the effect of birefringence on measurement accuracy when different polarization techniques are used in Fizeau interferometers. We demonstrate that measurement error is reduced dramatically and can be eliminated if the reference and test beams are circularly polarized rather than linearly polarized. © 2005 Optical Society of America

*OCIS codes:* 120.3180, 260.5430, 260.1440.

## 1. Introduction

In a common-path interferometer, e.g., a Fizeau interferometer, both the reference and the test beams go through the same optics up to the reference surface; therefore, any defect in the common path affects the phases of reference and test beams equally and has no effect on the measurement accuracy.<sup>1</sup> However, when the reference and test beams have different polarization states, if a component in the common path has residual birefringence, the reference and test beams will see different phases and an error will be introduced in the measurement. In this case the interferometer is no longer strictly common path, though physically it still is. There now exist commercial phase-shifting Fizeau interferometers that use this polarization technique to take multiple frames simultaneously to freeze vibration.<sup>2,3</sup> Birefringence is a concern because it is always present, especially for big and thick optics. For example, Schott Glass specifies the residual birefringence of specially annealed glass at  $<6$  nm/cm.<sup>4</sup> If a test plate is 10 cm thick, the birefringence is  $\sim 60$  nm, which is significant if the

required measurement accuracy is high. But, by using circularly polarized light instead of linearly polarized light, one can dramatically reduce and even eliminate the measurement error caused by the residual birefringence. In Section 2 we give the maximum measurement error when the reference and test beams are linearly polarized. In Section 3, first we set up a model with which to study the effect of birefringence when circularly polarized beams are used for the reference and test beams, and then we show analytically that the combined beam before phase shifting is elliptically polarized rather than linearly polarized. In Subsection 3.B we study the beam intensities after a general elliptically polarized beam passes the linear polarizer. We show that the observed intensity is sinusoidal, but a phase retardation is introduced and fringe contrast is reduced. We use this result in Subsection 3.C to analyze the phase measurement error that is due to birefringence. We present the simulation result in Subsection 3.D.

## 2. Linear Polarization

To analyze the effect of birefringence we assume a Fizeau interferometer as shown in Fig. 1. As in all Fizeau interferometers, the reference surface is the last surface in the system, so all the transmissive optics are common path. If some optics have residual birefringence, we model the combined birefringence as a wave plate whose fast axis and retardation vary from point to point in the pupil. The light reflected

The authors are with the College of Optical Sciences, the University of Arizona, 1630 East University Boulevard, Tucson, Arizona 85721. C. Zhao's e-mail address is czhao@optics.arizona.edu.

Received 13 May 2005; accepted 21 July 2005.

0003-6935/05/357548-06\$15.00/0

© 2005 Optical Society of America

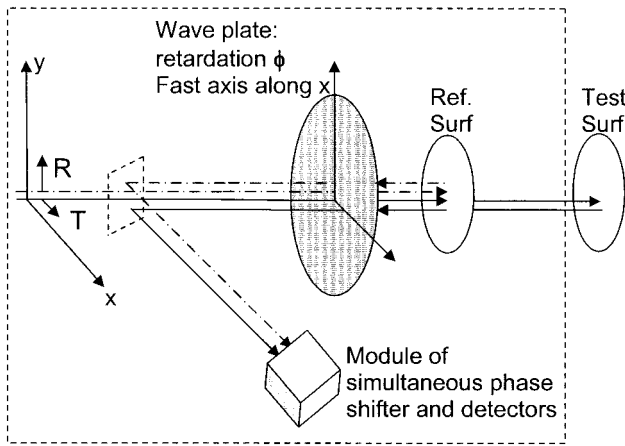


Fig. 1. Simultaneous phase-shifting polarization Fizeau interferometer. Ref. Surf, Test Surf, reference and test surfaces; R, T, reference and test beams, respectively.

from the reference surface creates the reference wavefront, and light transmitted through this surface and then reflected from the surface under test creates the test wavefront. The interference between the two is used to determine the error in the surface under test. Phase-shift interferometry is conventionally performed by moving the reference surface to cause a phase shift and capturing successive interferograms. Recently Fizeau interferometers that simultaneously capture all the different phase shifts were developed. These systems are configured such that the reference wavefront and the test wavefront have orthogonal polarization states. Through clever use of geometry or coherence, the system can be configured such that only the desired polarization states are measured.

If the reference and the test beams are linearly polarized, e.g., if the reference beam is  $x$  polarized and the test beam is  $y$  polarized, and if the residual birefringence is  $\phi$  (in radians) and its fast axis is along  $x$ , then the test beam sees an additional phase  $2\phi$  that is due to this birefringence. That additional phase is mistakenly attributed to the surface figure error:

$$\delta_{\max} = \frac{\phi}{2\pi}\lambda. \quad (1)$$

This would be the maximum measurement error caused by the residual birefringence in the common path of the reference and the test beams.

### 3. Circular Polarization

When the reference and the test beams are circularly polarized, a linear polarizer can be used as the phase shifter, as shown in Fig. 2. Rotation of the linear polarizer shifts the relative phase between the two polarizations.<sup>5</sup> 4D Technologies uses the same principle but a pixilated mask to achieve simultaneous phase shifting.<sup>3</sup>

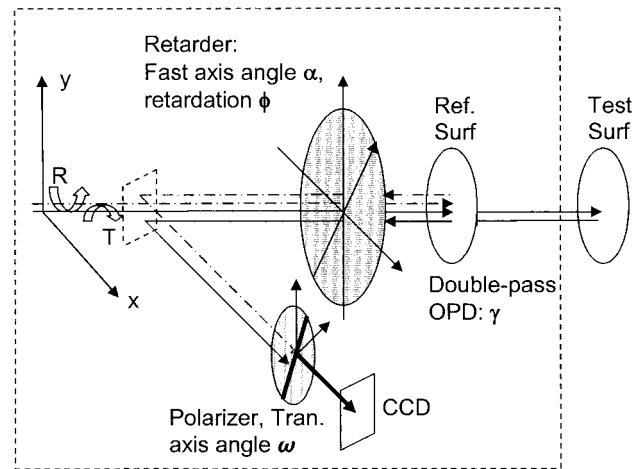


Fig. 2. Phase-shifting interferometer with circularly polarized reference and test beams uses a linear polarizer as the phase shifter. Tran, transmission; OPD, optical path difference.

#### A. Combined Beam before the Phase Shifter

If, for example, the test beam is right-hand circular and the reference beam is left-hand circular, there always exists a coordinate system in which the reference and test beams are in phase. We define this coordinate system as the global coordinate system  $X_G-Y_G$  (see Fig. 3). In this coordinate system, the Jones vectors<sup>6</sup> of the test beam (denoted  $T_G$ ) and of the reference beam (denoted  $R_G$ ) are

$$T_G = \begin{pmatrix} 1 \\ -i \end{pmatrix}, \quad R_G = \begin{pmatrix} 1 \\ i \end{pmatrix}. \quad (2)$$

As stated in Section 2, the residual birefringence is modeled as a wave plate. Assume that its retardation is  $\phi$  (angle) and that its fast axis makes angle  $\alpha$  with the global  $X_G$  axis. We choose its fast axis as the local  $x$  axis, denoted the  $X_T$  axis. In the local coordinates

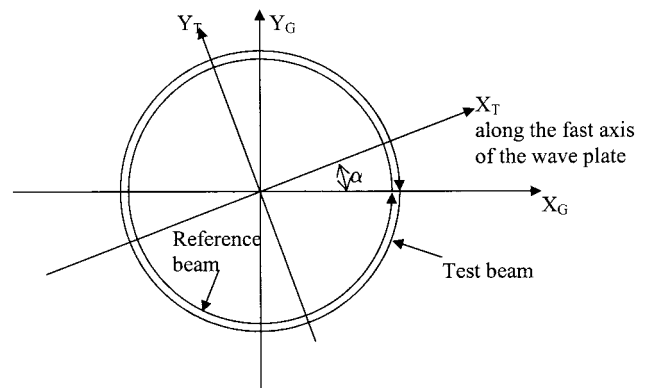


Fig. 3. Illustration of the definitions of the global coordinate system and the wave plate's local coordinate system.  $X_G-Y_G$  is the global coordinate system, in which the incident reference and test beams are in phase.  $X_T-Y_T$  is the wave plate local coordinate system with the fast axis along the  $X_T$  direction. The test and reference beams are circularly polarized and in phase in the global coordinate system. They have equal intensity (exaggerated in the figure).

$X_T$ - $Y_T$  (Fig. 3), the double-pass Jones matrix of the wave plate is

$$B_T = \begin{bmatrix} 1 & 0 \\ 0 & \exp(i2\phi) \end{bmatrix}. \quad (3)$$

In the wave plate's local coordinate system, the reference and the test beams see a phase shift:

$$T_T = \begin{pmatrix} 1 \\ -i \end{pmatrix} \exp(-i\alpha), \quad R_T = \begin{pmatrix} 1 \\ i \end{pmatrix} \exp(i\alpha). \quad (4)$$

After the light is reflected from the reference and the test surfaces and passes the wave plate a second time, the reference and test beams become, respectively,

$$T_T' = B_T T_T \exp(i2\gamma) = \begin{bmatrix} 1 \\ -i \exp(i2\phi) \end{bmatrix} \exp[i(2\gamma - \alpha)], \quad (5a)$$

$$R_T' = B_T R_T = \begin{bmatrix} 1 \\ i \exp(i2\phi) \end{bmatrix} \exp(i\alpha), \quad (5b)$$

where  $\gamma$  is the single-pass phase difference between the reference and test beams caused by the physical separation between reference and test surfaces along a ray.

The combined beam is

$$\begin{aligned} R_T' + T_T' &= \begin{Bmatrix} \exp[i(2\gamma - \alpha)] + \exp(i\alpha) \\ i \exp[i(2\phi + \alpha)] - i \exp[i(2\phi + 2\gamma - \alpha)] \end{Bmatrix} \\ &= \exp(i\gamma) \begin{bmatrix} 2 \cos(\gamma - \alpha) \\ 2 \sin(\gamma - \alpha) \exp(i2\phi) \end{bmatrix}. \end{aligned} \quad (6)$$

So, when there is no birefringence, i.e., when  $\phi = 0$ , the combined beam is linearly polarized with the electrical field vector oscillating along a direction that makes an angle  $\gamma - \alpha$  with the wave plate's local  $X_T$  axis and angle  $\gamma$  with the global  $X_G$  axis. When the residual birefringence is nonzero, the combined beam is elliptically polarized with phase difference  $2\phi$  between the  $E$  fields in the  $Y_T$  and  $X_T$  directions (see Fig. 4).

#### B. Intensity after an Elliptically Polarized Beam Passes the Phase Shifter

The reference and test beams both pass a linear polarizer before reaching the CCD. The polarizer combines the reference and test beams to obtain interference. It also serves as a phase shifter: When it rotates an angle of  $\omega$ , the phase difference between the reference and the test beams will increase by  $2\omega$ .<sup>5</sup> The interferometer can make simultaneous measurements with different phase shifts by creating multiple images of the pupil and viewing them through polarizers set at different angles.<sup>3</sup>

When a general elliptically polarized beam passes

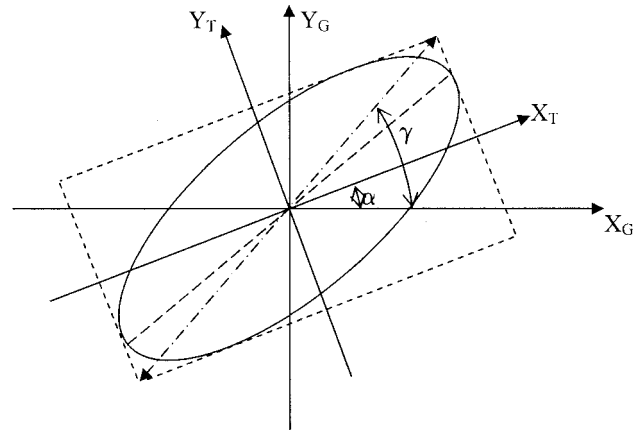


Fig. 4. Illustration of the combined beam's polarization. The dashed-dotted line illustrates the ideal linearly polarized beam when no birefringence exists; the solid ellipsis illustrates the elliptically polarized beam when birefringence exists.

through a linear polarizer, the transmitted beam's intensity is a function of the incident beam's parameters and the angle of the linear polarizer's transmission axis.

The Jones vector for general elliptically polarized light is

$$E = \begin{pmatrix} E_x \\ E_y \end{pmatrix} = \begin{bmatrix} A_x \\ A_y \exp(i\delta) \end{bmatrix}. \quad (7)$$

The electrical field vector at any point forms an ellipsis described by<sup>7</sup>

$$\left[ \frac{E_x}{A_x} \right]^2 + \left( \frac{E_y}{A_y} \right)^2 - 2 \left( \frac{E_x}{A_x} \right) \left( \frac{E_y}{A_y} \right) \cos(\delta) = \sin^2(\delta). \quad (8)$$

Define an angle  $\theta$  such that

$$\tan(\theta) = A_y/A_x. \quad (9)$$

Then the axis of the ellipsis forms an angle  $\psi$  with the  $x$  axis, as shown in Fig. 5, where

$$\tan(2\psi) = \tan(2\theta) \cos(\delta). \quad (10)$$

Assume that the elliptically polarized beam passes through a linear polarizer whose transmission axis makes an angle  $\omega$  with the  $x$  axis. The Jones matrix for the polarizer is

$$P = \begin{pmatrix} \cos^2 \omega & \cos \omega \sin \omega \\ \cos \omega \sin \omega & \sin^2 \omega \end{pmatrix}.$$

After the linear polarizer, the transmitted  $E$  field is

$$\begin{aligned} E_{\text{trans}} &= P \begin{bmatrix} A_x \\ A_y \exp(i\delta) \end{bmatrix} \\ &= [A_x \cos \omega + A_y \sin \omega \exp(i\delta)] \begin{pmatrix} \cos \omega \\ \sin \omega \end{pmatrix}. \end{aligned} \quad (11)$$

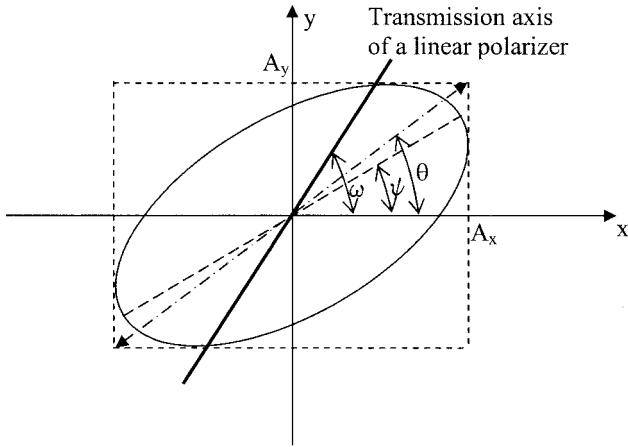


Fig. 5. Illustration of definitions of the angles  $\theta$  and  $\psi$  associated with elliptically polarized light. Also shown is a linear polarizer with a transmission axis that forms angle  $\omega$  with the  $x$  axis.

The intensity of the beam is

$$I = |E_{\text{trans}}|^2 = 1/2(A_x^2 + A_y^2) + 1/2[A_x^4 + 2A_x^2A_y^2 \times \cos(2\delta) + A_y^4]^{1/2} \cos(2\omega - 2\Psi), \quad (12)$$

where again  $\tan(2\Psi) = \tan(2\theta) \cos(\delta)$ .

Equation (12) demonstrates that we can measure  $\psi$ , which is a characteristic of the incident elliptically polarized beam, by phase-shifting interferometry with a linear polarizer as a phase shifter. When the incident beam is linearly polarized, i.e., when  $\delta = 0$ , then  $\Psi = \theta$ . When the beam is elliptically polarized compared to the linear polarization case, the beam intensity as a function of  $\omega$  sees a phase shift:

$$2\Delta = 2(\theta - \Psi). \quad (13)$$

From Eq. (12) we also obtain the fringe contrast

$$C = \frac{[A_x^4 + 2A_x^2A_y^2 \cos(2\delta) + A_y^4]^{1/2}}{A_x^2 + A_y^2}. \quad (14)$$

With the definition of  $\theta$ , the fringe contrast can be rewritten as

$$C = [1 - \sin^2(2\theta)\sin^2\delta]^{1/2}. \quad (15)$$

Figure 6 plots the transmitted beam intensity as a function of  $\omega$  for a linearly polarized beam and an elliptically polarized beam.

### C. Analysis

In Subsection 3.A we showed that, when birefringence exists, the combined beam from reference and test surfaces is elliptically polarized [Eq. (6)]. In Subsection 3.B we showed that we still measure a phase by using phase-shifting interferometry but with an error [Eqs. (12) and (13)]. The error depends on the

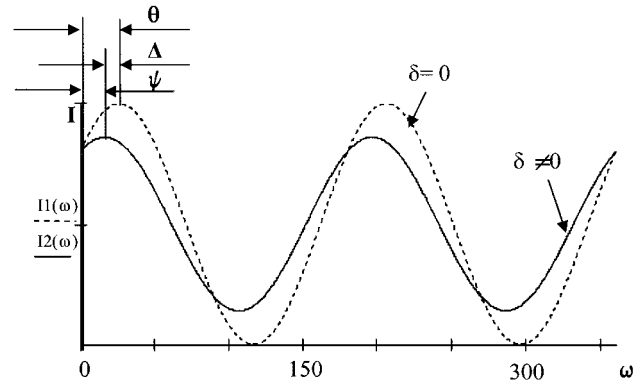


Fig. 6. Transmitted light intensity as a function of the linear polarizer's rotation angle after the wave plate converts circular to linear polarization. Dashed curve, no error and linearly polarized light. Solid curve, birefringence has caused the light to be elliptically polarized. Note that the intensity has a phase shift and less contrast when the incident beam is elliptically polarized than when it is linearly polarized.

characteristic of the elliptically polarized beam. From Eqs. (6), (10), and (13) we get

$$\tan(2\Delta) = \tan(2\theta - 2\Psi) = \frac{2 \tan[2(\gamma - \alpha)] \sin^2 \phi}{1 + \tan^2[2(\gamma - \alpha)] \cos 2\phi}, \quad (16)$$

which indicates that surface measurement error  $\Delta$  is a function of retardation  $\phi$ , birefringence angle  $\alpha$ , and actual phase  $\gamma$ . Because this error is a function of phase  $\gamma$ , it will vary when this phase is changed by making slight adjustments to the system.

Assume that

$$-\frac{\pi}{4} < \phi < \frac{\pi}{4};$$

then the maximum phase measurement error is

$$\tan(2\Delta_{\text{max}}) = \frac{\sin^2 \phi}{\sqrt{\cos 2\phi}}. \quad (17)$$

For a small  $\phi$  approximation,

$$2\Delta_{\text{max}} \approx \phi^2. \quad (18)$$

The maximum surface figure measurement error is then

$$\delta_{\text{max}} = \frac{\Delta_{\text{max}}}{2\pi} \lambda \approx \frac{\phi^2}{4\pi} \lambda, \quad (19)$$

which indicates that the maximum measurement error has a quadratic dependence on the amount of birefringence.

For comparison, in Fig. 7 we plot the maximum

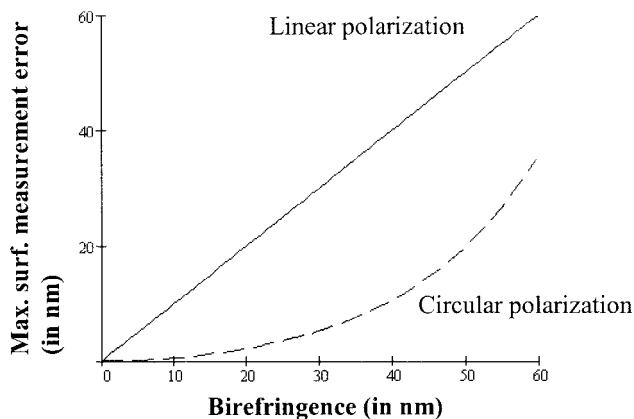


Fig. 7. Maximum surface measurement error versus birefringence for both linear and circular polarization.

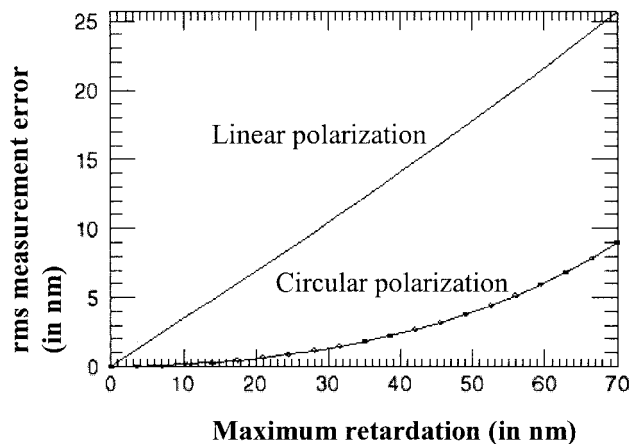


Fig. 9. Plot of rms surface measurement error as a function of maximum retardation of the birefringence distribution shown in Fig. 8(a) for both linear and circular polarization. Circles, results of theoretical calculation by use of Eq. (16), which agree with the interferometric simulation results for circular polarization.

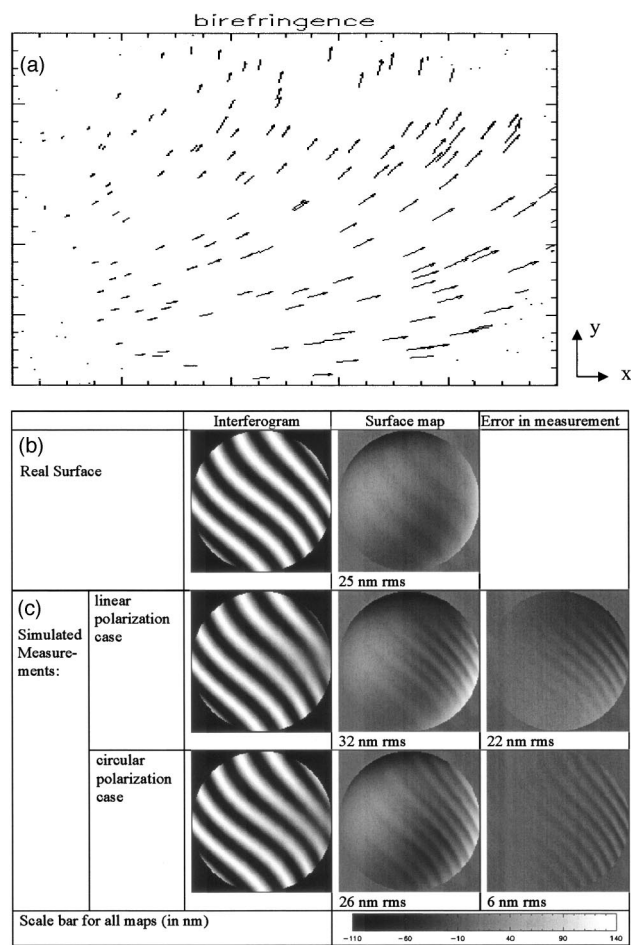


Fig. 8. Simulated Fizeau measurements for a system with birefringence in the common part of the system. (a) Birefringence map. The fast-axis angle has a linear distribution along the  $y$  axis from  $0^\circ$  to  $90^\circ$  and the retardation has a linear distribution along the  $x$  axis from 0 to 60 nm. (b) Results of simulation for an ideal system with 25 nm rms surface irregularity. (c) Results for simulated phase-shift interferometry for 60 nm birefringence and the spatial distribution shown in (a). We calculated the measurement error by subtracting the ideal surface error from the simulated measurement. Note the reduction in fringe contrast as well as the phase error for both cases.

surface measurement errors as a function of birefringence when the reference and test beams are linearly and circularly polarized, respectively, for a small amount of residual birefringence.

#### D. Simulation of Surface Measurements for a System with Birefringence

The effect of birefringence is illustrated by a set of simulations. We perform the analysis for an interferometer that has a 10 cm thick transmissive optic with a birefringence of 6 nm/cm. A map of the birefringence is shown in Fig. 8(a). We evaluate the performance of this system as it measures a mirror that has 25 nm rms surface irregularities. We also assume that the measurements are made with five fringes of tilt owing to alignment. The ideal and measured surface maps and measurement error maps are shown in Fig. 8(b). The results verify that the measurement error is significantly smaller for small residual birefringence when circularly polarized beams, rather than linearly polarized beams, are used.

If we maintain the distribution of birefringence and vary the magnitude of retardation, we expect to see the measurement error increase as a function of maximum retardation. Figure 9 shows the rms measurement error as a function of the maximum retardation for linear and circular polarization. It is obvious that measurement error is linear to birefringence when linearly polarized beams are used. In contrast, the measurement error is quadratic to birefringence when circularly polarized beams are used instead.

There is an important distinction between the forms of the measurement errors for the two cases. When linear polarization is used, an error is created that will be proportional to the birefringence and will be constant for all interferograms. Superimposed is an error that depends on the alignment and shows up as ripples in the surface with two times the frequency of the interferogram fringes. This component of the

error will change as the alignment is adjusted and thus can be reduced by averaging, but the larger, fixed component would remain as a real error in the test. For circular polarization there is no fixed error, and only the ripple type that depends on the interferogram alignment. Therefore it is possible to reduce the effect of the birefringence for the case of circular polarization by averaging multiple maps with different alignments.

#### 4. Summary

Fizeau interferometers can use polarization techniques to create a phase shift between reference and test beams. If some element in the common path exhibits residual birefringence, it can limit measurement accuracy. We model the residual birefringence as a wave plate whose fast-axis orientation and retardation vary from point to point in the pupil. If the reference and test beams are linearly polarized and orthogonal, the measurement phase error can be as large as the amount of birefringence. We studied the case when the two beams are circularly polarized and orthogonal, and we derived a set of relations with which to calculate the measurement error and the fringe contrast when birefringence is present. For a small amount of birefringence, we showed that the error is quadratic to the amount of birefringence. So, in the case of small birefringence, the measurement

error is significantly smaller if circular polarization rather than linear polarization is used to differentiate reference and test beams. In addition, this error is a function of the phase difference between the reference and the test, so one can further reduce the error by averaging multiple measurements with slight phase shifts.

#### References

1. M. V. R. K. Murty, "Newton, Fizeau, and Haidinger interferometers," in *Optical Shop Testing*, D. Malacara, ed. (Wiley, 1978), pp. 1–45.
2. For example, see [www.4dtechnology.com](http://www.4dtechnology.com) (FizCam series of interferometers) or [www.engsynthesis.com](http://www.engsynthesis.com) (Intellium H1000 Fizeau interferometer).
3. J. Millerd, N. Brock, M. North-Morris, M. Novak, and J. Wyant, "Pixelated phase-mask dynamic interferometer," in *Interferometry XII: Techniques and Analysis*, K. Creath and J. Schmit, eds., Proc. SPIE **5531**, 304–314 (2004).
4. See Information, p. 16 of the Schott Glass catalog at [http://www.us.schott.com/optics\\_devices/english/download/catalog\\_optical\\_glass\\_informations\\_usa\\_2003.pdf](http://www.us.schott.com/optics_devices/english/download/catalog_optical_glass_informations_usa_2003.pdf).
5. G. Jin, N. Bao, and P. S. Chung, "Applications of a novel phase-shift method using a computer controlled polarization mechanism," *Opt. Eng.* **33**, 2733–2737 (1994).
6. E. Hecht, *Optics* (Addison-Wesley Longman, 1998), pp. 368–371.
7. M. Born and E. Wolf, *Principles of Optics* (Pergamon, 1980), pp. 25–32.